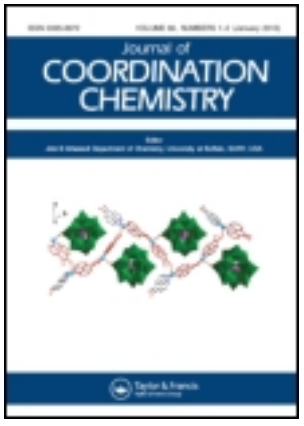

Journal of Coordination Chemistry
Publication details, including instructions for authors and subscription information:
http://www.tandfonline.com/loi/gcoo20

Synthesis, structure, DNA-binding, and cytotoxic activities of N-(5-chloro-2-hydroxyphenyl)-N′-[3-(2-hydroxyethylamino)propyl]oxamide and its dicopper(II) complex

Shi-Hao Cui [a], Man Jiang [b], Yan-Tuan Li [a], Zhi-Yong Wu [c] & Xiao-Wen Li [c]

[a] Marine Drug & Food Institute, Ocean University of China, 5 Yushan Road, Qingdao, 266003, PR China

[b] Qindao Municipal Medical Group, Qindao, Shandong, 266011, PR China

[c] Key Laboratory of Marine Drug, Chinese Ministry of Education, Ocean University of China, Qingdao, PR China

Published online: 22 Nov 2011.

To cite this article: Shi-Hao Cui, Man Jiang, Yan-Tuan Li, Zhi-Yong Wu & Xiao-Wen Li (2011) Synthesis, structure, DNA-binding, and cytotoxic activities of N-(5-chloro-2-hydroxyphenyl)-N′-[3-(2-hydroxyethylamino)propyl]oxamide and its dicopper(II) complex, Journal of Coordination Chemistry, 64:23, 4209-4224, DOI: 10.1080/00958972.2011.638063

To link to this article: http://dx.doi.org/10.1080/00958972.2011.638063

Journal of Coordination Chemistry
Vol. 64, No. 23, 10 December 2011, 4209–4224

Synthesis, structure, DNA-binding, and cytotoxic activities of *N*-(5-chloro-2-hydroxyphenyl)-*N′*-[3-(2-hydroxyethylamino) propyl]oxamide and its dicopper(II) complex

SHI-HAO CUI†, MAN JIANG‡, YAN-TUAN LI*†, ZHI-YONG WU§ and XIAO-WEN LI§

†Marine Drug & Food Institute, Ocean University of China, 5 Yushan Road, Qingdao, 266003, PR China
‡Qindao Municipal Medical Group, Qindao, Shandong, 266011, PR China
§Key Laboratory of Marine Drug, Chinese Ministry of Education, Ocean University of China, Qingdao, PR China

(*Received 13 August 2011; in final form 20 October 2011*)

A dissymmetrical *N*,*N′*-*bis*(substituted)oxamide, *N*-(5-chloro-2-hydroxyphenyl)-*N′*[3-(2-hydroxyethylamino)propyl]oxamide (H_3oxpep), and its dicopper(II) complex, $[Cu_2(oxpep)(phen)]ClO_4$ (**1**) (phen = 1,10-phenanthroline), were synthesized. The crystal structure of **1** was determined by single-crystal X-ray diffraction. In **1**, Cu1 and Cu2 are bridged by *cis*-oxpep^{3-} with Cu···Cu separation of 5.2007(6) Å. Cu1 is in a distorted square-pyramidal environment, while Cu2 has a square-planar coordination geometry. The 3-D supramolecular structure of **1** is formed through π–π stackings and hydrogen bonds. The DNA-binding properties and cytotoxic activities of the two compounds were investigated. The results suggest that the two compounds can interact with *HS*-DNA by intercalation with binding affinities following the order **1** > H_3oxpep, which is consistent with their anticancer activities.

Keywords: Dissymmetrical *N*,*N′*-*bis*(substituted)oxamide; Dicopper(II) complex; Crystal structure; DNA-binding property; Cytotoxic activity

1. Introduction

Deoxyribonucleic acid (DNA) plays an important role in cells since it contains all the genetic information for cellular function. Although there are numerous biological targets in cancer cells, including DNA, RNA, enzyme, and other protein receptors, it is generally accepted that DNA is the primary target for many anticancer drugs [1, 2]. Cisplatin is a widely used anticancer drug [3, 4] and the detailed molecular mechanism of its action has been elucidated, which involves covalent binding to DNA [5]. Although it is curative in some tumor types, its usage is limited by both side-effects and acquired cellular resistance [6]. Hence, more-efficacious, target-specific, less-toxic, and non-covalently DNA-binding

*Corresponding author. Email: yantuanli@ouc.edu.cn

ISSN 0095-8972 print/ISSN 1029-0389 online © 2011 Taylor & Francis
http://dx.doi.org/10.1080/00958972.2011.638063

anticancer drugs are required to be developed. Inspired by cisplatin, number of researchers now focus on the development of new metal-based anticancer drugs targeting DNA with non-covalent binding modes. Transition-metal complexes can bind to DNA non-covalently by intercalation, electrostatic interaction, and groove binding. These binding modes are important in the development of drugs, new biochemical tools, etc. Many complexes possessing these binding modes have been synthesized and studied for DNA-binding properties and cytotoxic activities [7–9].

Copper is a biologically relevant element and many enzymes depend on copper for their activities. Copper(II) complexes also possess numerous biological activities, such as antitumor [10], antimicrobial [11], DNA cleavage [12], DNA, and protein binding [13] activities. Among the above biological activities, attention has been paid to the research of DNA-binding properties and cytotoxic activities since copper(II) complexes are regarded as promising alternatives to cisplatin [13]. Compared with the number of studies dealing with mononuclear copper complexes [7, 12, 13], relatively few studies on binuclear copper complexes have been reported [14, 15]. *N*,*N*′-*bis*(substituted)oxamides are good candidates as bridging ligands in forming di- or polynuclear complexes because they have potential coordination sites that permit the formation of metal complexes. Coordination abilities toward metal ions can be modified and tuned by changing the nature of the amide substituents [16, 17]. A series of complexes with symmetrical *N*,*N*′-*bis*(substituted)oxamides as bridging ligands have been reported [18–20]. However, studies on complexes of dissymmetrical *N*,*N*′-*bis*(substituted) oxamides are limited [21], due to synthetic difficulty. Exploration of interactions between complexes and DNA stimulates us to synthesize new dicopper(II) complexes with bridging dissymmetrical *N*,*N*′-*bis*(substituted)oxamides to evaluate and understand the factors in DNA-binding properties and cytotoxic activities.

Herein, we report the synthesis, structure, DNA-binding properties, and cytotoxic activities of a dissymmetrical *N*,*N*′-*bis*(substituted)oxamide, *N*-(5-chloro-2-hydroxyphenyl)-*N*′-[3(2-hydroxyethylamino)propyl]oxamide (H_3oxpep), and its dinuclear copper(II) complex, $[Cu_2(oxpep)(phen)]ClO_4$ (**1**), which was structurally characterized by X-ray crystallography.

2. Experimental

2.1. *Materials*

All chemicals used in the synthesis were of reagent grade and obtained commercially without purification. Doubly-distilled water was used to prepare buffers. Ethidium bromide (EB) and herring sperm DNA (*HS*-DNA) were purchased from Sigma Corp. and used as received.

2.2. *Synthesis of H_3oxpep*

A total of 2.22 mL (20 mmol) of ethyl oxalyl chloride in 10 mL THF (tetrahydrofuran) was added dropwise into a 40 mL THF solution containing 2.86 g (20 mmol) of 2-amino-4-chlorophenol at 0°C. The mixture was stirred for 2 h at room temperature. Then, the mixture was added dropwise into solution which contained 30 mL of absolute ethanol

and 4.8 mL (40 mmol) of 2-(3-amino-propylamino)ethanol at 0°C with stirring. The resulting solution was stirred for 5 h at room temperature. H_3oxpep, precipitated as yellow powder, was recrystallized from ethanol and dried under vacuum. Yield: 88%. Anal. Calcd for $C_{13}H_{18}N_3O_4Cl$ (%): C, 49.45; H, 5.75; N, 13.31. Found (%): C, 49.55; H, 5.61; N, 13.32. MS(ES-MS), m/z (%): 316.1 (100) $[MH]^+$. ^{1}H NMR (DMSO-d_6, 600 MHz): δ 9.82 (br, 1 H), δ 9.26 (t, $J = 5.52$ Hz, 1H), δ 8.15 (s, 1H), δ 6.96 (d, $J = 8.82$ Hz, 1H), δ 6.81 (d, $J = 8.82$ Hz, 1H), δ 5.58 (br, 2H), δ 3.48 (t, $J = 6.06$, Hz, 2H), δ 3.25 (dt, $J = 5.52$, 6.06 Hz, 2H), δ 2.65-2.61 (m, 4H), δ 2.50 (quintet, $J = 1.80$ Hz, 1H), δ 1.67 (quintet, $J = 6.60$ Hz, 2H).

2.3. *Synthesis of 1*

A total of 0.0315 g (0.1 mmol) of H_3oxpep was dissolved in 5 mL of methanol and deprotonated by 0.0255 g (0.3 mmol) of piperidine in 2 mL of methanol. To this solution, a 5 mL methanol solution of 1,10-phenanthroline (0.1 mmol, 0.0180 g) was added. After stirring for 10 min, a solution of $Cu(ClO_4)_2 \cdot 6H_2O$ (0.2 mmol, 0.0742 g) in 5 mL methanol was further added dropwise. The mixture was stirred vigorously at 60°C for 6 h, and then filtered. The filtrate was allowed to stand at room temperature for several days to give dark brown crystals. Yield: 60%. Anal. Calcd for $Cu_2C_{25}H_{23}Cl_2N_5O_8$ (%): C, 41.73; H, 3.22; N, 9.73. Found (%): C, 41.65; H, 3.25; N, 9.84.

2.4. *Physical measurements*

Carbon, hydrogen, and nitrogen analyses were performed with a Perkin-Elmer elemental analyzer Model 240. The mass spectrum (ES–MS) was measured with a Waters Q-TOF GLOBLE mass spectrometer. ^{1}H NMR spectrum was measured on a JEOL JNM-ECP600 spectrometer with TMS as an internal standard when DMSO-d_6 was used as solvent. Molar conductance was measured with a Shanghai DDS-11 A conductometer. The infrared spectrum was recorded with samples as KBr pellets in a Nicolet model Impact 470 FTIR spectrophotometer. The UV-Vis spectrum was recorded in a 1 cm path length quartz cell on a Cary 300 spectrophotometer. Fluorescence was tested on an Fp-750w fluorometer. Viscosity measurements were carried out using an Ubbelodhe viscometer immersed in a thermostated water bath maintained at 16.0(±0.1)°C.

2.5. *Crystal structure determination of 1*

The X-ray diffraction experiment for **1** was conducted on a Bruker APEX area-detector diffractometer with graphite monochromated Mo-Kα radiation ($\lambda = 0.71073$ Å) at 296 K. The crystal structure was solved by direct methods followed by Fourier synthesis. Structure refinements were performed by full matrix least-squares using SHELXL-97 on F^2 [22]. The oxygens in perchlorate and the carbons in hydroxyethylaminopropyl (heap) group of $oxpep^{3-}$ are both disordered into two parts. The occupancies of the two perchlorates were equal to 0.5, while those of heap were refined freely at first and then fixed at 0.75 (suffix A) and 0.25 (suffix B), respectively. The hydrogen of hydroxyl was located in a difference Fourier map and refined freely.

The Cl–O lengths of ClO_4^- were limited to 1.4 Å with DFIX and the O···O distances were restrained by SADI instruction for the reasonable geometry. The C–O, C–N, and C–C in heap were similarly restrained by DFIX instruction to 1.43, 1.47, and 1.54 Å, respectively. The other hydrogen atoms were placed in calculated positions with C–H = 0.97 (methylene), 0.93 Å (aromatic) and N–H = 0.91 Å, and included in the final cycles of refinement in the riding mode, with $U_{iso}(H) = 1.2\,U_{eq}$ of the carrier atoms. Crystal data and structural refinement parameters for **1** are summarized in table 1 and selected bond distances and angles are listed in tables 2 and 3.

2.6. *DNA-binding experiments*

All experiments involving herring sperm DNA (*HS*-DNA) were performed in *tris*-(hydroxymethyl)aminomethane-HCl (Tris-HCl) buffer solution (pH = 7.16). Tris-HCl buffer was prepared using deionized and sonicated triply-distilled water. Solution of *HS*-DNA in Tris-HCl buffer gave a ratio of UV absorbance at 260 and 280 nm, A_{260}/A_{280}, of *ca* 1.9, indicating that the DNA was sufficiently free of protein [23]. The concentration of *HS*-DNA was determined according to its absorbance at 260 nm adopting $\epsilon_{260} = 6600\,(\text{mol L}^{-1})^{-1}\,\text{cm}^{-1}$ [24]. All stock solutions of *HS*-DNA were stored at 4°C and used after no more than 4 days. Concentrated stock solutions of H_3oxpep and **1** were prepared by dissolving in DMSO and suitably diluted with Tris-HCl buffer to required concentrations for all the experiments. Electronic absorption spectral titration experiments were performed keeping concentrations of the two compounds constant while varying the *HS*-DNA concentration. Equal solution of *HS*-DNA was added to every solution of H_3oxpep, **1**, and the reference to eliminate the absorbance of

Table 1. Crystal data and details of the structure determination for **1**.

Empirical formula	$Cu_2C_{25}H_{23}N_5O_8C_{l2}$
Formula weight	719.46
Crystal system	Monoclinic
Space group	$P2_1/c$
Unit cell dimensions (Å, °)	
a	12.9484(7)
b	23.8073(14)
c	8.8829(5)
α	90.00
β	105.5880(10)
γ	90.00
Volume (Å^3), Z	2637.6(3), 4
Calculated density (g cm^3)	1.812
Absorption coefficient (mm^{-1})	1.877
F(0 0 0)	1456
Crystal size (mm^3)	0.07 × 0.09 × 0.31
Temperature (K)	296
Wavelength (Å)	0.71073
Limiting indices	$-16 \le h \le 14$; $-31 \le k \le 19$; $-11 \le l \le 11$
Reflections collected	15,525
Independent reflection	6030[R(int) = 0.038]
θ range for data collection (°)	1.84–27.57
Observed data [$I > 2\sigma(I)$]	3983
R, wR_2, S	0.0400, 0.0984, 1.02
Max., avg. shift/error	0.000, 0.000

HS-DNA itself. In the ethidium bromide (EB) fluorescence displacement experiment, 5 μL of the EB Tris-HCl solution (1 mmol L^{-1}) was added to 1 mL of *HS*-DNA solution (at saturated binding levels) [25] and stored in the dark for 2 h before use. Then solution of each compound was titrated into the DNA/EB mixture and diluted in Tris-HCl buffer to 5 mL, producing solutions with varied mole ratio of each compound to *HS*-DNA. Before measurement, the mixture was shaken up and incubated at room temperature for 30 min. Fuorescence spectra bound to *HS*-DNA were obtained at an emission wavelength of 581 nm in the Fluorometer. Viscosity experiments were performed using an Ubbelodhe viscometer immersed in a thermostated water bath maintained at 16.0(±0.1)°C. *HS*-DNA samples of approximately 200 base pairs in length were prepared by sonication in order to minimize complexities arising from DNA flexibility [26]. Flow times were measured with a digital stopwatch, each compound was measured thrice, and an average flow time was calculated. Relative viscosities for *HS*-DNA in the presence and absence of each compound were calculated from the relation $\eta = (t - t_0)/t_0$, where t is the observed flow time of DNA-containing solution and t_0 is that of Tris-HCl buffer alone. Data were presented as $(\eta/\eta_0)^{1/3}$ *versus* binding ratio [27], where η is the viscosity of DNA in the presence of H_3oxpep or **1** and η_0 is the viscosity of DNA alone.

2.7. *In vitro antitumor activity evaluation by SRB assays*

In vitro antitumor activities of H_3oxpep, **1**, and cisplatin were evaluated against two cancer cell lines, including SMMC-7721 and A549, by using the Sulforhodamine B

Table 2. Selected bond distances (Å) and angles (°) for **1**.

Cu1–O1	1.981(2)	Cu1–O4	2.402(3)
Cu1–N1	1.955(3)	Cu1–N2	1.980(3)
Cu1–N3	1.998(3)	Cu2–O2	1.964(2)
Cu2–O3	1.904(2)	Cu2–N4	1.975(3)
Cu2–N5	1.983(3)	CL1–C4	1.740(3)
O1–Cu1–O4	93.52(9)	O1–Cu1–N1	82.55(9)
O1–Cu1-N2	159.54(10)	O1–Cu1–N3	97.98(9)
O4–Cu1–N1	105.56(10)	O4–Cu1–N2	104.20(10)
O4–Cu1–N3	77.02(10)	N1–Cu1–N2	82.88(11)
N1–Cu1–N3	177.35(11)	N2–Cu1–N3	95.96(11)
O2–Cu2–O3	86.55(9)	O2–Cu2–N4	98.36(10)
O2–Cu2–N5	173.82(10)	O3–Cu2–N4	173.77(11)
O3–Cu2–N5	91.60(11)	N4–Cu2–N5	83.12(11)

Table 3. Hydrogen-bonding geometries for **1** (Å, °).

D–HA	*D*–H	H···A	*D*···A	*D*–H···A
O4–H4···O1^{i}	0.91	1.82(4)	2.705(3)	165(2)
C14–H14···O6A	0.93	2.46	3.142(11)	130.3
C14–H14···O6B	0.93	2.50	3.211(10)	133.6
C15–H15···O7A	0.93	2.57	3.339(11)	140.7
C15–H15···O8B	0.93	2.45	3.305(9)	153.2
C16–H16···O7A^{ii}	0.93	2.44	3.271(11)	148.1
C16–H16···O8B^{ii}	0.93	2.46	3.362(12)	162.9

Symmetry codes: ^{i}x, ½ − y, −1/2 + z; ^{ii}−x, −y, −z.

(SRB) assays. All cells were cultured in RPMI 1640 supplemented with 10% (v/v) fetal bovine serum, 1% (w/v) penicillin (104 U mL^{-1}), and 10 mg mL^{-1} streptomycin. Cell lines were maintained at 37°C in a 5% (v/v) CO_2 atmosphere with 95% (v/v) humidity. Cultures were passaged weekly using trypsin-EDTA to detach the cells from their culture flasks. The three compounds were dissolved in DMSO and diluted to the required concentration with culture medium when used. The content of DMSO in the final concentrations did not exceed 0.1%. At this concentration, DMSO was found to be non-toxic to the cells tested. Rapidly growing cells were harvested, counted, and incubated at the appropriate concentration in 96-well microplates for 24 h. The compounds dissolved in culture medium were then applied to the culture wells to achieve final concentrations ranging from 10^{-3} to 102 μg mL^{-1}. Control wells were prepared by the addition of culture medium without cells. The plates were incubated at 37°C in a 5% CO_2 atmosphere for 48 h. Upon completion of the incubation, the cells were fixed with ice-cold 10% trichloroacetic acid (100 mL) for 1 h at 4°C, washed five times in distilled water and allowed to dry in air, and stained with 0.4% SRB in 1% acetic acid (100 mL) for 15 min. The cells were washed four times in 1% acetic acid and air-dried. The stain was solubilized in 10 mmol L^{-1} unbuffered Tris base (100 mL) and the OD of each well was measured at 540 nm on a microplate spectrophotometer. The IC_{50} values were calculated from the curves constructed by plotting cell survival (%) *versus* the complex concentration (μg mL^{-1}).

3. Results and discussion

3.1. *Synthetic routes and general properties of H_3oxpep and 1*

In general, two synthetic strategies are available for the preparation of binuclear complexes. The first is to use a designed polynucleating ligand, which offers coordination geometry or ligand field strength suitable for metal ions. The second is to use a complex as "ligand" that contains a potential donor group capable of coordinating to another metal ion. In this study, our aim was to obtain a μ-oxamido-bridged dicopper(II) complex, therefore, the first synthetic strategy was adopted. For that, a new dissymmetrical *N*,*N*′-*bis*(substituted)oxamide, *N*-(5-chloro-2hydroxyphenyl)-*N*′-[3-(2-hydroxyethylamino)propyl]oxamide (H_3oxpep), was chosen as bridging ligand. Simultaneously, 1,10-phenanthroline (phen) was used as terminal ligand. In the course of preparing the dicopper(II) complex, the use of piperidine as base makes the bridging ligand coordinate to copper(II) through deprotonated oxamido nitrogen. Elemental analyses indicate that the reaction of H_3oxpep with $Cu(ClO_4)_2 \cdot 6H_2O$ and phen in 1 : 2 : 1 ratio yields the dicopper(II) complex $[Cu_2(oxpep)(phen)]ClO_4$ (**1**), as expected. The synthetic pathway for H_3oxpep and **1** may be represented by scheme 1.

Both H_3oxpep and **1** are insoluble in non-polar solvents, moderately soluble in water and methanol, and very soluble in DMF and DMSO to give stable solutions at room temperature. In the solid state, the two compounds are fairly stable in air to allow physical measurements. The molar conductance value (81 $\Omega^{-1}cm^{-2}mol^{-1}$) of **1** in DMF solution falls in the expected range for 1 : 1 electrolyte [28]. These observations coincide with the following spectral characterization.

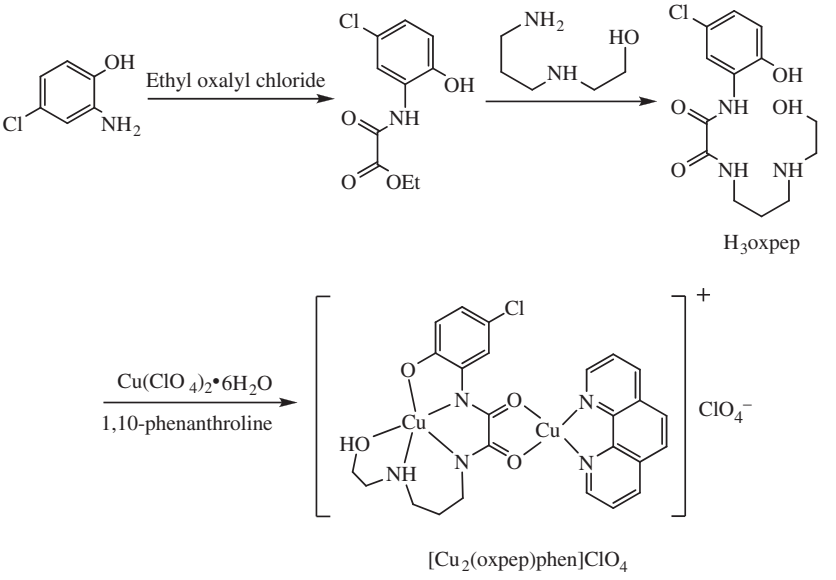

Scheme 1. Synthesis of H_3oxpep and **1**.

3.2. *IR and electronic spectra*

The IR spectra were taken from 4000 to 400 cm^{-1}. The carbonyl stretching vibration at 1657 cm^{-1} for H_3oxpep is considerably shifted to lower frequency 1629 cm^{-1} in **1**, implying that the carbonyl oxygens of H_3oxpep take part in coordination. This shift has often been used as proof of an oxamido-bridge [29]. The ν(C=N) at 1523 for phen is found in **1**, indicating the coordination of phen to copper(II) [30]. A broad and intense band centered at 1108 cm^{-1}, and a strong sharp band at 628 cm^{-1} for the antisymmetric stretching vibration and the antisymmetric bending vibration of non-coordinated perchlorate [31] are also observed for **1**.

The UV-Vis absorption spectra of H_3oxpep and **1** were measured in the UV-Vis region (200–800 nm) using DMSO as solvent. For H_3oxpep, there is an intense band at 229 nm which can be assigned to the π–π* transition of the substituted benzene. In the spectrum of **1**, four absorption bands with varied intensities are observed. The three bands at 229, 269, and 288 nm can be assigned to π–π* transitions of coordinated $oxpep^{3-}$ and phenanthroline [32, 33]. A broad band is observed at 671 nm in the spectrum of **1**, corresponding to the d–d transition of copper(II) [34].

3.3. *Crystal structure of 1*

As shown in figure 1, two copper(II) ions are bridged by *cis*-$oxpep^{3-}$ and the Cu···Cu separation through the oxamido-bridge is 5.2007(6) Å. The *cis*-oxamido group coordinates to Cu1 and Cu2 in the usual chelating mode, with bite angles of 82.89(10) and 86.55(9)°, respectively. Cu1 is in a distorted square-pyramidal coordination geometry with a τ value of 0.30 [35], while Cu2 has a square-planar coordination geometry. Cu1 resides in an inner site of the *cis*-$oxpep^{3-}$ and the basal plane is formed by O1, N1, N2, and N3 from $oxpep^{3-}$. The maximum displacement from the coordination plane is

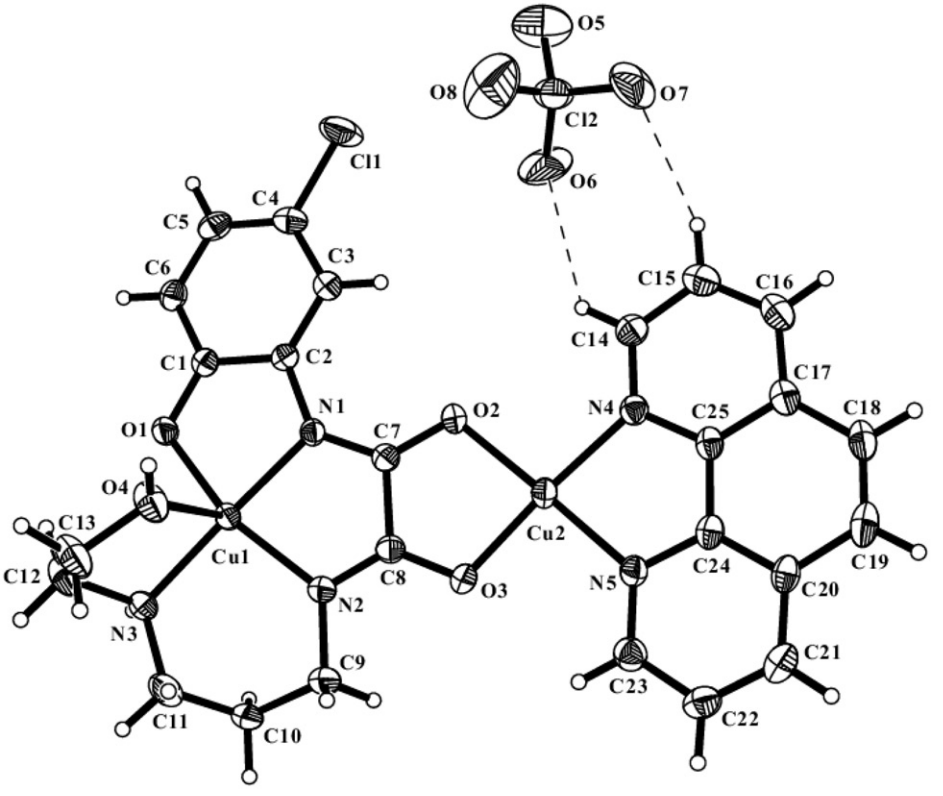

Figure 1. A view of 1 with the atom numbering scheme. Displacement ellipsoids are drawn at 30% probability and hydrogen atoms are shown as small spheres of arbitrary radii. Dashed lines indicate non-classical hydrogen bonds.

0.1175(14) Å (N1). Cu1 displaces 0.1469(13) Å out of the plane. The apical position is occupied by O4 with Cu1–O4 distance of 2.402(2) Å, which is longer than the equatorial one (Cu1–O1: 1.981(2) Å). Cu2 coordinates to the *exo*-oxygens (O3 and O4) of the *cis*-oxpep^{3-} and nitrogens (N4 and N5) from phenanthroline. Maximum deviation of O3, O4, N4, and N5 from basal plane is 0.022(16) Å (N5) and Cu2 is 0.08(6) Å out of the plane. The *cis*-oxpep^{3-} coordinates pentadentate to Cu1 and results in the formation of three five-membered rings and one six-membered ring.

In the crystal structure, two kinds of π–π stacking interactions connect the complex molecules, forming 1-D chains parallel to the *c* axis (figure 2). One is observed between a phenanthroline and another one at $1-x$, $-y$, $-z^{iii}$. The nearest separation is 3.338(4) Å for C14^{iii} to the N5-pyridine ring of phenanthroline. The other is observed between the quinoline ring of phenanthroline and the substituted benzene ring of oxpep^{3-} with the symmetry operation of $1-x$, $-y$, $1-z^{iv}$. The nearest separation is 3.318(4) Å for C6^{iv} to the middle benzene ring of phenanthroline. These 1-D chains are linked through classical hydrogen bonds O4–H4$\cdots$O1^{i} [symmetry code: ^{i}x, $\frac{1}{2}-y$, $-1/2+z$] into a 2-D network parallel to the plane b0c. Adjacent layers are further assembled by relatively weak non-classical hydrogen bonds C16–H16$\cdots$O7^{ii} [symmetry code: $^{ii}-x$, $-y$, $-z$] to form a 3-D supramolecular structure which is revealed in figure 3.

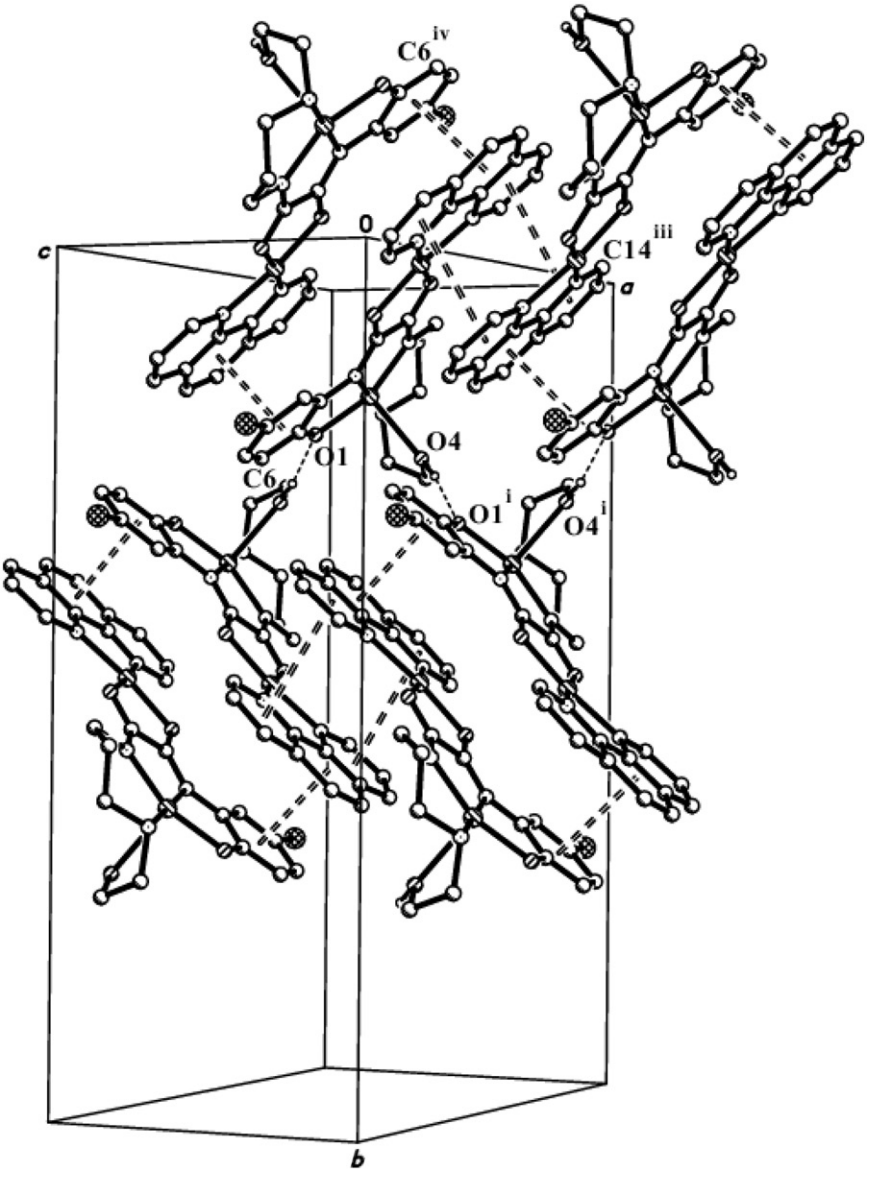

Figure 2. A 2-D network of **1** parallel to the *b*0*c* plane, formed by classical O4–H4 $\cdots$ O1^{i} hydrogen bonds (dashed lines) and two kinds of π–π stacking interactions (double dashed lines). The ClO_4^{-1} and hydrogen atoms not involved in hydrogen bonds have been omitted for clarity. [Symmetry codes: ^{i}x, $\frac{1}{2}-y$, $-1/2+z$; $^{iii}1-x$, $-y$, $-z$; $^{iv}1-x$, $-y$, $1-z$].

3.4. *DNA-binding studies*

3.4.1. Electronic absorption titration. The application of electronic absorption spectrometry in DNA-binding studies is one of the most useful techniques to examine the binding mode and strength of a compound to DNA. Usually, the binding of an intercalative molecule to DNA is accompanied by hypochromism and red-shift in the

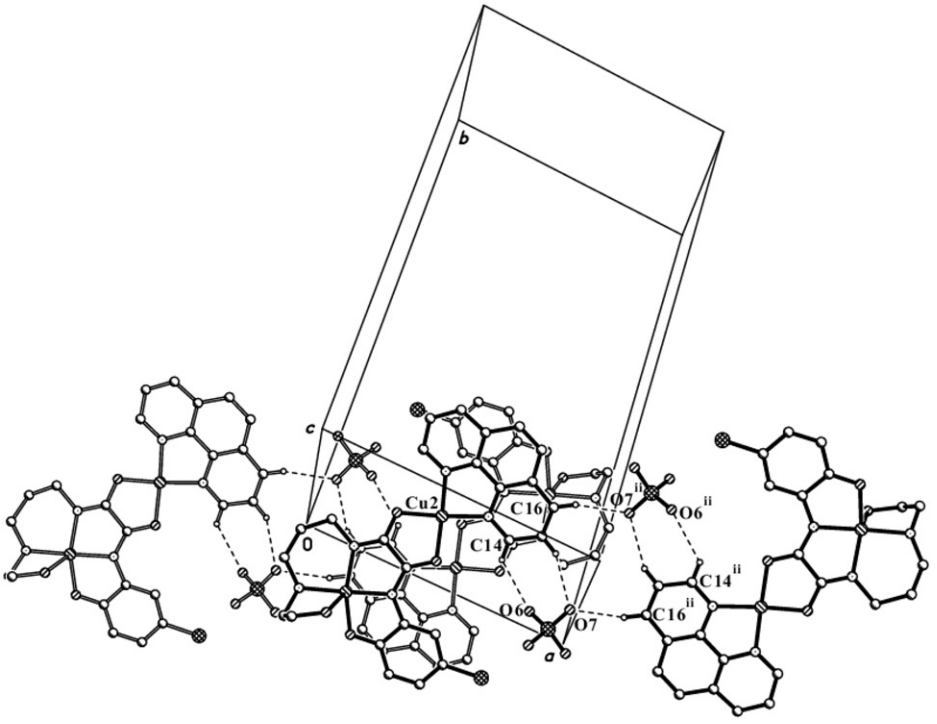

Figure 3. A view of the non-classical hydrogen bonds in **1** (dashed lines). Hydrogen atoms not involved in hydrogen bonds have been omitted for clarity. [Symmetry codes: $^{ii}-x, -y, -z$].

absorption spectrum due to stacking interactions between aromatic chromophores of the molecule and DNA base pairs. The extent of hypochromism and red-shift are commonly proportional to the intercalative binding strength [36, 37]. The absorption spectra of H_3oxpep and **1** in the absence and presence of *HS*-DNA are given in figure 4. As shown in figure 4, absorption spectra of H_3oxpep and **1** at 229 nm show hypochromic (7.9% for H_3oxpep and 10.9% for **1**) and red-shift of 3 nm on the addition of increasing amounts of *HS*-DNA. According to electronic absorption spectra, we can deduce that both H_3oxpep and **1** bind to DNA by intercalation.

In order to further evaluate the binding strength of H_3oxpep and **1** with *HS*-DNA, the intrinsic binding constants K_b were determined by monitoring changes in absorbance at 229 nm adopting the following equation [38]:

$$[\mathrm{DNA}]/(\varepsilon_a - \varepsilon_f) = [\mathrm{DNA}]/(\varepsilon_b - \varepsilon_f) + 1/K_b(\varepsilon_b - \varepsilon_f) \quad (1)$$

where [DNA] is the concentration of DNA, ε_a, ε_f, and ε_b correspond to the extinction coefficients, respectively, for each addition of DNA to the compounds, for the free compounds, and for the compounds in fully bound form. From the $[\mathrm{DNA}]/(\varepsilon_a - \varepsilon_f)$ *versus* [DNA] plots (insets in figure 4), the binding constants for H_3oxpep and **1** are estimated to be 6.67×10^4 $(\mathrm{mol\,L^{-1}})^{-1}$ ($R = 0.9951$ for six points) and 4.50×10^5 $(\mathrm{mol\,L^{-1}})^{-1}$ ($R = 0.9934$ for six points), respectively. The better binding constant of **1** than H_3oxpep may be due to the phenanthroline ring in **1** which is expected to be

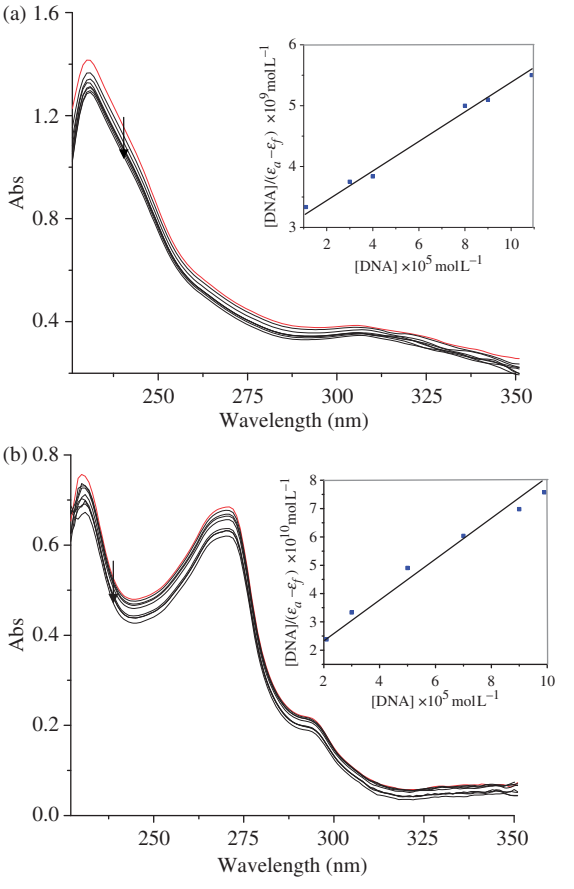

Figure 4. Absorption spectra of H_3oxpep (a) and **1** (b) upon titration of *HS*-DNA. Arrows indicate changes upon increasing *HS*-DNA concentration. Insets: Plots of $[DNA]/(\varepsilon_a - \varepsilon_f)$ *vs.* [DNA] for absorption titration of *HS*-DNA to H_3oxpep (a) and **1** (b).

stacked between base pairs upon interaction with DNA. Electrostatic interaction may be another factor for **1** to enhance the binding strength to DNA, which is lacking in H_3oxpep [39]. Comparing the intrinsic binding constant of **1** with those of some mononuclear copper(II) complexes containing 1,10-phenanthroline (table 4), we conclude that **1** can strongly bind to DNA and its binding constant is remarkable. Furthermore, the K_b value of **1** is also higher than those of some dicopper(II) complexes containing 1,10-phenanthroline, such as $[Cu_2(pdmp)(phen)](ClO_4)_2$ [31], $Cu_2(phen)_2Cl_4$ [33], and $[Cu_2(bipp)(phen)_2](ClO_4)_4$ [46], as listed in table 4. The main differences between these dicopper(II) complexes are in their bridging ligands and this indicates that diverse bridging ligands have a profound effect on DNA-binding ability, as revealed by the different binding constants.

3.4.2. Fluorescence titration. In order to further investigate the interactions between the two compounds and *HS*-DNA, the ethidium bromide (EB) fluorescence displacement experiments were employed. Ethidium bromide (EB) is a well-known fluorescence

Table 4. The intrinsic binding constants (K_b) with DNA.

Compound	K_b ($(\text{mol L}^{-1})^{-1}$)	Reference
H_3oxpep	6.67×10^4	This work
Complex **1**	4.50×10^5	This work
$Cu(phen)_2Cl_2$	2.75×10^3	[40]
$[Cu(l\text{-leucine})(phen)(H_2O)]NO_3$	5.10×10^3	[41]
$[Cu(l\text{-isoleucine})(phen)(H_2O)]NO_3$	2.24×10^3	[41]
$[Cu(l\text{-proline})(phen)(H_2O)]ClO_4$	3.86×10^3	[42]
$[Cu(l\text{-tyrosine})(phen)]ClO_4$	4.08×10^3	[43]
$[Cu(l\text{-threonine})(phen)(H_2O)]ClO_4$	6.35×10^3	[44]
[Cu(HisLeu [a])(phen)]Cl	4.20×10^3	[45]
[Cu(HisSer [b])(phen)]Cl	4.90×10^3	[45]
Cu(saltyr [c])(phen)	3.47×10^4	[30]
[Cu(tdp [d])(phen)]$ClO_4 \cdot CH_3OH$	0.90×10^5	[7]
$[Cu_2(pdmp$ [e]$)(phen)](ClO_4)_2$	4.40×10^4	[31]
$Cu_2(phen)_2Cl_4$	4.75×10^4	[33]
$[Cu_2(bipp$ [f]$)(phen)_2](ClO_4)_4$	1.60×10^4	[46]

[a]HisLeu = histidylleucine.
[b]HisSer = histidylserine.
[c]Saltyr = salicylidene tyrosine.
[d]Htdp = 2-[(2-(2-hydroxyethylamino)ethylimino)methyl]phenol.
[e]pdmp = 6,6′-piprazine-1,4-diyl-dimethylene *bis*(4-methyl phenol).
[f]bipp = 2,9-*bis*(2-imidazo[4,5-f][1,10]phenanthroline)-1,10-phenanthroline.

probe that can bind to DNA [47]. In general, the fluorescence intensity of DNA is very low, and that of EB in Tris-HCl buffer is also not high because of being quenched by the solvent molecules. But when EB is intercalated into DNA base pairs, the fluorescence intensity is greatly increased. The fluorescence can be quenched by the addition of another molecule [39, 48] owing to the replacement of EB fluorophores. Thus, EB can be used to probe the interactions of compounds with DNA.

In our experiment, as illustrated in figure 5, the fluorescence intensity of EB bound to *HS*-DNA at 581 nm shows obvious decreasing trend upon increasing the concentration of **1**, indicating that **1** can bind to *HS*-DNA, and some EB molecules are released into solution. Similar trend was also observed for H_3oxpep (figure 5). The fluorescence quenching of EB bound to *HS*-DNA by the two compounds is in agreement with the linear Stern–Volmer equation [49]:

$$I_0/I = 1 + K_{sv}[Q] \quad (2)$$

where I_0 and I represent the fluorescence intensities in the absence and presence of quencher, respectively. K_{sv} is a linear Stern-Volmer quenching constant, Q is the concentration of quencher. In the Stern–Volmer plots (insets in figure 5), K_{sv} values are given by the slopes. The K_{sv} values for H_3oxpep and **1** are 3.42×10^4 ($R = 0.9942$ for 11 points) and 9.75×10^4 ($R = 0.9972$ for 11 points), respectively. The quenching ability of the two compounds to the EB-DNA system follows the order: **1** > H_3oxpep. The data show that the DNA-binding interaction of **1** is stronger than that of H_3oxpep, consistent with the above electronic absorption spectral results.

3.4.3. Viscosity measurement. Viscosity measurement is sensitive to length changes and regarded as the least ambiguous and the most critical test of DNA-binding modes in solution, providing reliable evidence for intercalative binding [50, 51]. To further

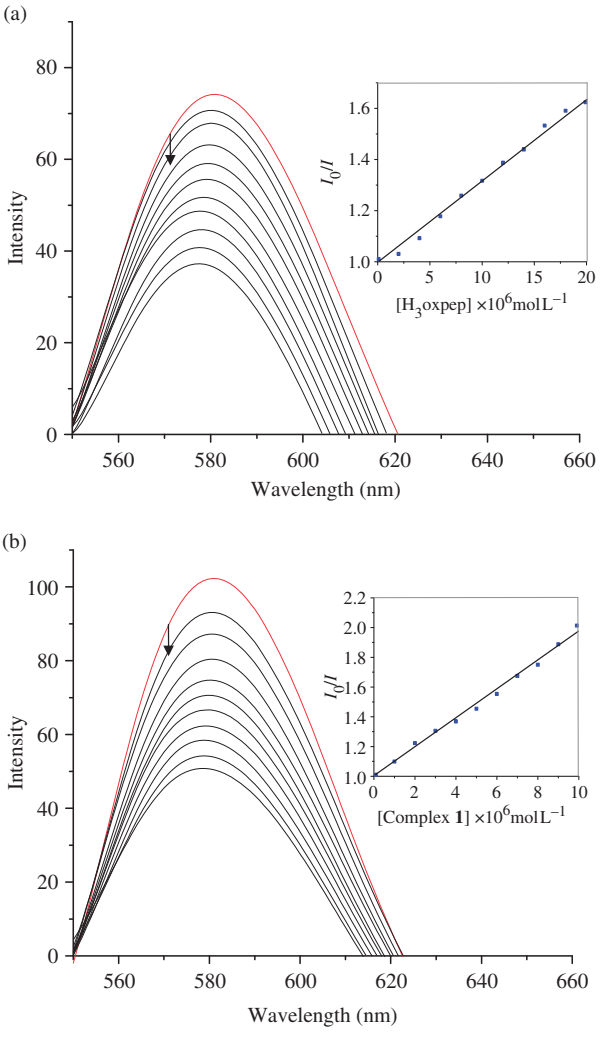

Figure 5. Emission spectra of *HS*-DNA-EB system upon titration of H_3oxpep (a) and **1** (b). Arrows show the changes upon increasing concentrations of the two compounds. Insets: Plots of I_0/I *vs*. [compound] for the titration of H_3oxpep (a) and **1** (b) to the *HS*-DNA-EB system.

clarify the binding modes of the two compounds with *HS*-DNA, viscosity studies were carried out. For either compound, the relative viscosity of *HS*-DNA increased with the increasing concentration of H_3oxpep or **1** (figure 6). The increase of viscosity can be ascribed to the extension of *HS*-DNA resulting from intercalation of H_3oxpep or **1** between adjacent DNA base pairs. The increased degree of viscosity follows the order: **1** > H_3oxpep. The obviously increased viscosity by **1** may arise from the phenanthroline ring which makes it intercalate more deeply into *HS*-DNA base pairs than H_3oxpep. Thus, the results of viscosity studies validate those obtained from electronic absorption titration and fluorescence titration.

If we compare the DNA-binding of **1** with some structurally-similar polynuclear copper(II) complexes reported earlier by us, using *N*,*N*′-*bis*(substituted)oxamides as

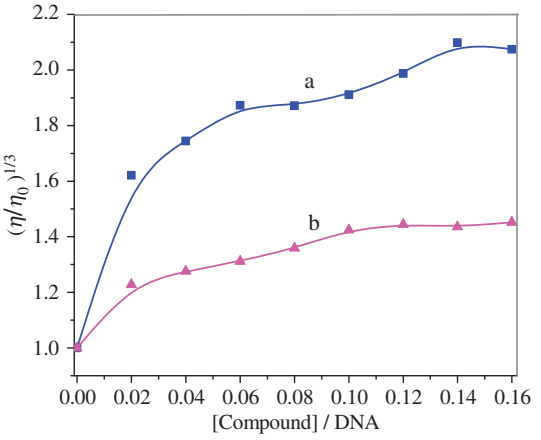

Figure 6. Effects of the increasing amounts of **1** (a) and H_3oxpep (b) on the relative viscosity of *HS*-DNA at 16.0(±0.1)°C, [*HS*-DNA] = 0.2 mmolL^{-1}.

Table 5. *In vitro* antitumor activities against SMMC-7721 and A549.

	IC_{50} (μg mL^{-1})	
Compound	SMMC-7721	A549
H_3oxpep	>100	>100
Complex 1	32.1 ± 0.1	28.0 ± 0.2
Cisplatin	5.4 ± 0.2 ng mL^{-1}	7.6 ± 0.4 ng mL^{-1}

bridging ligands and polypyridines as terminal ligands [52, 53], we find that not only the interaction modes but also the DNA-binding ability of these μ-oxamido-bridged polynuclear complexes are different. These results confirm that interactions of this class of complexes toward *HS*-DNA may be tuned by changing the bridging or terminal ligands. Such strategy should be important in designing new μ-oxamido-bridged polynuclear complexes and understanding the binding properties between oxamido complexes and DNA. Indeed, further investigations using various bridging and terminal ligands are still required in order to confirm the effect and are in progress in our laboratory.

3.5. In vitro *antitumor activity studies*

In vitro antitumor activities of H_3oxpep and **1** against two cancer cell lines, human hepatocellular carcinoma cell line SMMC-7721 and human lung adenocarcinoma cell line A549, were investigated in comparison with the widely used drug cisplatin by using SRB assays. As revealed in table 5, though **1** has higher IC_{50} values than those of cisplatin, the inhibition of cell proliferation produced by **1** is still rather active with its IC_{50} values falling in the 28–32 μg mL^{-1} range, and better than those of H_3oxpep. The cytotoxicities of compounds vary with the planarity of different ligands and the extent of their intercalation into DNA base pairs [7, 54, 55] and the significant cytotoxicity of **1** may be partially attributed to its strong intercalation.

4. Conclusions

In order to investigate the interactions of binuclear complexes with DNA, we synthesized and structurally characterized a new μ-oxamido-bridged dicopper(II) complex $[Cu_2(oxpep)(phen)]ClO_4$ (**1**) by employing *N*-(5-chloro-2-hydro-xyphenyl)-*N*′ [3-(2-hydroxyethylamino)propyl]oxamide (H_3oxpep) as bridging ligand and 1,10-phenanthroline (phen) as terminal ligand. DNA-binding properties of the two compounds were studied through absorption and emission spectrometry and viscometry. Both compounds interact with *HS*-DNA by intercalation. The DNA-binding ability of **1** is better than free H_3oxpep, which can be attributed to the electrostatic and stronger stacking interactions between **1** and DNA. Complex **1** has higher DNA-binding constant than some known copper(II) complexes containing 1,10-phenanthroline. The cytotoxicities of H_3oxpep and **1** against SMMC-7721 and A549 cell lines were tested *in vitro* by SRB assays. Complex **1** has good cytotoxicity, which may be partially explained by strong intercalation. These results should be valuable in designing new μ-oxamido-bridged polynuclear complexes and understanding the DNA-binding properties and anticancer activities of this class of complexes.

Supplementary material

Crystallographic data for the structural analysis of the copper(II) complex has been deposited with the Cambridge Crystallographic Data Center, CCDC No. 823655. Copies of this information may be obtained free of charge from The Director, CCDC, 12 Union Road, Cambridge, CB2 1EZ, UK (Fax: C44 1233 336 033; Email: deposit@ccdc.cam.ac.uk).

Acknowledgments

This project was supported by the National Natural Science Foundation of China (No. 21071133), the Natural Science Foundation of Qingdao City (No. 09-1-3-73-jch), and the Program for Changjiang Scholars and Innovative Research Team in University (IRT0944).

References

[1] C.X. Zhang, S.J. Lippard. *Curr. Opin. Chem. Biol.*, **7**, 481 (2003).
[2] C.H. Wu, D.H. Wu, X. Liu, G. Guoyiqibayi, D.D. Guo, G. Lv, X.M. Wang, H. Yan, H. Jiang, Z.H. Lu. *Inorg. Chem.*, **48**, 2352 (2009).
[3] T. Boulikas, M. Vougiouka. *Oncol. Rep.*, **10**, 1663 (2003).
[4] E. Wong, C.M. Giandomenico. *Chem. Rev.*, **99**, 2451 (1999).
[5] E.R. Jamieson, S.J. Lippard. *Chem. Rev.*, **99**, 2467 (1999).
[6] D. Wang, S.J. Lippard. *Nat. Rev. Drug Discov.*, **4**, 307 (2005).
[7] V. Rajendiran, R. Karthik, M. Palaniandavar, V.S. Periasamy, M.A. Akbarsha, B.S. Srinag, H. Krishnamurthy. *Inorg. Chem.*, **46**, 8208 (2007).

[8] L. Messori, F. Abbate, G. Marcon, P. Orioli, M. Fontani, E. Mini, T. Mazzei, S. Carotti, T. Connell, P. Zanello. *J. Med. Chem.*, **43**, 3541 (2000).
[9] J. Liu, W.J. Zheng, S. Shi, C. Tan, J. Chen, K. Zheng, L. Ji. *J. Inorg. Biochem.*, **102**, 193 (2008).
[10] M. Chauhan, K. Banerjee, F. Arjmand. *Inorg. Chem.*, **46**, 3072 (2007).
[11] J.D. Saha, U. Sandbhor, K. Shirisha, S. Padhye, D. Deobagkar, C.E. Ansond, A.K. Powelld. *Bioorg. Med. Chem. Lett.*, **14**, 3027 (2004).
[12] R. Ren, P. Yang, W. Zheng, Z. Hua. *Inorg. Chem.*, **39**, 5454 (2000).
[13] S.S. Bhat, A.A. Kumbhar, H. Heptullah, A.A. Khan, V.V. Gobre, S.P. Gejji, V.G. Puranik. *Inorg. Chem.*, **50**, 545 (2011).
[14] C.Y. Gao, X.F. Ma, J. Lu, Z.G. Wang, J.L. Tian, S.P. Yan. *J. Coord. Chem.*, **64**, 2157 (2011).
[15] N. Raman, A. Sakthivel, R. Jeyamurugan. *J. Coord. Chem.*, **63**, 1080 (2010).
[16] R. Ruiz, J. Faus, F. Lloret, M. Julve, Y. Journaux. *Coord. Chem. Rev.*, **193**, 1069 (1999).
[17] M.C. Dul, E. Pardo, R. Lescouezec, Y. Journaux, J. Ferrando-Soria, R. Ruiz-Garcia, J. Cano, M. Julve, F. Lloret, D. Cangussu, C.L.M. Pereira, H.O. Stumpf, J. Pasan, C. Ruiz-Perez. *Coord. Chem. Rev.*, **254**, 2281 (2010).
[18] Z.L. Liu, L.C. Li, D.Z. Liao, Z.H. Jiang, S.P. Yan. *Cryst. Growth Des.*, **5**, 783 (2005).
[19] E.Q. Gao, H.Y. Sun, D.Z. Liao, Z.H. Jiang, S.P. Yan. *Polyhedron*, **21**, 359 (2002).
[20] Y.H. Zhang, M. Yu, Q.L. Wang, G.F. Xu, M. Hu, G.M. Yang, D.Z. Liao. *Polyhedron*, **27**, 3371 (2008).
[21] X.W. Zhang, Y.J. Zheng, Y.T. Li, Z.Y. Wu, C.W. Yan. *J. Coord. Chem.*, **63**, 2985 (2010).
[22] G.M. Sheldrick. *Acta Cryst.*, **A64**, 112 (2008).
[23] J. Marmur. *J. Mol. Biol.*, **3**, 208 (1961).
[24] M.E. Reichmann, S.A. Rice, C.A. Thomas, P.J. Doty. *J. Am. Chem. Soc.*, **76**, 3047 (1954).
[25] J.B. Chaires, N. Dattagupta, D.M. Crothers. *Biochemistry*, **21**, 3933 (1982).
[26] G. Cohen, H. Eisenberg. *Biopolymers*, **8**, 45 (1969).
[27] J.K. Barton, J.M. Goldberg, C.V. Kumar, N.J. Turro. *J. Am. Chem. Soc.*, **108**, 2081 (1986).
[28] W.J. Geary. *Coord. Chem. Rev.*, **7**, 81 (1971).
[29] H. Ojima, K. Nonoyama. *Coord. Chem. Rev.*, **85**, 92 (1988).
[30] P.R. Reddy, A. Shilpa. *Polyhedron*, **30**, 565 (2011).
[31] S. Anbu, M. Kandaswamy. *Polyhedron*, **30**, 123 (2011).
[32] L.F. Chin, S.M. Kong, H.L. Seng, K.S. Khoo, R. Vikneswaran, S.G. Teoh, M. Ahmad, S.B.A. Khoo, M.J. Maah, C.H. Ng. *J. Inorg. Biochem.*, **105**, 221 (2011).
[33] Q.Q. Zhang, F. Zhang, W.G. Wang, X.L. Wang. *J. Inorg. Biochem.*, **100**, 1344 (2006).
[34] P. Camurlu, A. Yilmaz, L. Tatar, D. Kisakürek, D. Ülkü. *Cryst. Res. Technol.*, **40**, 271 (2005).
[35] A.W. Addison, T.N. Rao, J. Reedijk, J.V. Rijin, G.C. Verschoor. *J. Chem. Soc., Dalton Trans.*, 1349 (1984).
[36] D. Cremer, J.A. Pople. *J. Am. Chem. Soc.*, **97**, 1354 (1975).
[37] T.M. Kelly, A.B. Tossi, D.J. McConnell, T.C. Strekas. *Nucleic Acids Res.*, **13**, 6017 (1985).
[38] A. Wolf, G.H. Shimer Jr, T. Meehan. *Biochemistry*, **26**, 6392 (1987).
[39] Y.T. Li, C.Y. Zhu, Z.Y. Wu, M. Jiang, C.W. Yan. *J. Coord. Chem.*, **62**, 3795 (2009).
[40] T. Gupta, S. Dhar, M. Nethaji, A.R. Chakravarty. *J. Chem. Soc., Dalton Trans.*, 1896 (2004).
[41] R. Rao, A.K. Patra, P.R. Chetana. *Polyhedron*, **27**, 1343 (2008).
[42] P.R. Reddy, N. Raju, P. Manjula, K.V.G. Reddy. *Chem. Biodiv.*, **4**, 1565 (2007).
[43] S. Ramakrishnan, V. Rajendiran, M. Palaniandavar, V.S. Periasamy, B.S. Srinag, H. Krishnamurthy, M.A. Akbarsha. *Inorg. Chem.*, **48**, 1309 (2009).
[44] S.C. Zhang, Y.G. Zhu, C. Tu, H.Y. Wei, Z. Yang, L.P. Lin, J. Ding, J.F. Zhang, Z.J. Guo. *J. Inorg. Biochem.*, **98**, 2099 (2004).
[45] P.R. Reddy, P. Manjula. *Chem. Biodiv.*, **4**, 468 (2007).
[46] J.Z. Wu, L. Yuan, J.F. Wu. *J. Inorg. Biochem.*, **99**, 2211 (2005).
[47] J. Olmsted, D.R. Kearns. *Biochemistry*, **16**, 3647 (1977).
[48] E.B. Veale, T. Gunnlaugsson. *J. Org. Chem.*, **75**, 5513 (2010).
[49] O. Stern, M. Volmer. *Z. Phys.*, **20**, 183 (1919).
[50] S. Satyanarayana, J.C. Dabrowiak, J.B. Chaires. *Biochemistry*, **31**, 9319 (1992).
[51] L. Jin, P. Yang. *J. Inorg. Biochem.*, **68**, 79 (1997).
[52] H.H. Lu, Y.J. Zheng, Y.T. Li, Z.Y. Wu, K. Zheng, C.W. Yan. *J. Coord. Chem.*, **64**, 1360 (2011).
[53] X.W. Li, M. Jiang, Y.T. Li, Z.Y. Wu, C.W. Yan. *J. Coord. Chem.*, **63**, 1582 (2010).
[54] A. Barve, A. Kumbhar, M. Bhat, B. Joshi, R. Butcher, U. Sonawane, R. Joshi. *Inorg. Chem.*, **48**, 9120 (2009).
[55] J.H. Tan, Y.J. Lu, Z.S. Huang, L.Q. Gu, J.Y. Wu. *Eur. J. Med. Chem.*, **42**, 1169 (2007).